Journal of Energy Chemistry 26 (2017) 815–819

Contents lists available at ScienceDirect

Journal of Energy Chemistry

journal homepage: www.elsevier.com/locate/jechem

http://www.journals.elsevier.com/journal-of-energy-chemistry/

Carbon-coated manganese dioxide nanoparticles and their enhanced electrochemical properties for zinc-ion battery applications

Saiful Islam, Muhammad Hilmy Alfaruqi, Jinju Song, Sungjin Kim, Duong Tung Pham, Jeonggeun Jo, Seokhun Kim, Vinod Mathew, Joseph Paul Baboo, Zhiliang Xiu, Jaekook Kim*

Department of Materials Science and Engineering, Chonnam National University, 300 Yongbong-dong, Bukgu, Gwangju 61186, Republic of Korea

ARTICLE INFO

Article history:
Received 23 November 2016
Revised 6 April 2017
Accepted 7 April 2017
Available online 21 April 2017

Keywords:
Carbon coating
Manganese dioxide
Zinc-ion battery
Electrochemical properties

ABSTRACT

In this study, we report the cost-effective and simple synthesis of carbon-coated α-MnO_2 nanoparticles (α-MnO_2@C) for use as cathodes of aqueous zinc-ion batteries (ZIBs) for the first time. α-MnO_2@C was prepared via a gel formation, using maleic acid ($C_4H_4O_4$) as the carbon source, followed by annealing at low temperature of 270 °C. A uniform carbon network among the α-MnO_2 nanoparticles was observed by transmission electron microscopy. When tested in a zinc cell, the α-MnO_2@C exhibited a high initial discharge capacity of 272 mAh/g under 66 mA/g current density compared to 213 mAh/g, at the same current density, displayed by the pristine sample. Further, α-MnO_2@C demonstrated superior cycleability compared to the pristine samples. This study may pave the way for the utilizing carbon-coated MnO_2 electrodes for aqueous ZIB applications and thereby contribute to realizing high performance eco-friendly batteries.

1. Introduction

Since manganese dioxide (MnO_2) is relatively cheap, environmentally benign, and electrochemically active, it is considered as a promising energy storage electrode material. Different crystallographic polymorphs of MnO_2 namely α, ß, γ, δ, and λ can be obtained by different synthetic routes [1]. Among all these polymorphs, α-MnO_2 has a distinctive [2 × 2] tunnel structure and it has received much attention. In our previous report, α-MnO_2 nanorods were investigated as zinc-ion battery (ZIB) cathodes. This electrode showed a first discharge capacity of 233 mAh/g at 83 mA/g current density [2]. However, capacity fading under prolonged cycles, which has also been reported by many other groups, is a major drawback of this electrode [3,4]. Additionally, the intrinsically poor electrical conductivity of MnO_2 impedes the electronic path way and consequently, limits its electrochemical performance [4,5].

Naturally abundant, low-cost, and environmentally benign highly conducting materials, such as carbon can be used to overcome the aforementioned limitation of MnO_2. Carbon-coated electrode materials such as transition metal oxides have been widely studied to obtain high performance electrodes [6–9]. Hashem et al. prepared carbon-coated rod-shaped MnO_2 in order to achieve an electrode material with enhanced electrochemical performance for lithium-ion battery (LIB) application [10]. Incorporation of carbon materials including carbon nanotubes, graphene, and fullerene into MnO_2 increases its surface area and enhances its conductivity because of the formation of a MnO_2/C composite. Hence, these composite materials have been used in high performance supercapacitors and LIBs [11,12]. Mesoporous MnO_2/C spheres with a very large surface area (324 $m^2\ g^{-1}$) have been synthesized and investigated as an active electrode by Pan et al. [13]. Kim et al. demonstrated the electrochemical performance of an electrodeposited mesoporous MnO_2/C composite electrode for advanced supercapacitors [14]. Moreover, Li et al. reported on carbon coated MnO_2 nanorods obtained via a facile solid state grinding and low temperature calcination as a high performance electrode for supercapacitors [6]. Therefore, from the above discussion, it is clear that the carbon coating strategy is an effective method of improving conductivity and increasing the stability of electrode materials.

Here, for the first time, we report the enhanced electrochemical performance of carbon-coated α-MnO_2 nanoparticles for ZIBs. We have successfully prepared carbon-coated α-MnO_2 nanoparticles by just stirring α-MnO_2 nanoparticles in an ethanolic solution of maleic acid at a mild temperature until a gel is formed and finally it is annealed at lower temperature under Ar atmosphere. The carbon coatings on the electrode material not only increase the electrical conductivity and discharge capacity but also improve the electrode cycleability and capacity retention by preventing manganese dissolution from the active material during electrochemical discharge reaction. Higher discharge capacity and improved

* Corresponding author.
E-mail addresses: jaekook@chonnam.ac.kr, jaekook@jnu.ac.kr (J. Kim).

http://dx.doi.org/10.1016/j.jechem.2017.04.002

cycleability were obtained for the prepared carbon-coated MnO_2 sample.

2. Experimental

The pristine α-MnO_2 nanoparticles were synthesized before preparing the carbon-coated α-MnO_2 nanoparticles (α-MnO_2@C). First, 150 mmol of $Mn(CH_3COO)_2{\cdot}4H_2O$ was dissolved in 30 mL of distilled water (denoted: solution A). Then, a 50 mL solution of 100 mmol $KMnO_4$ was added dropwise to solution A. A dark brown precipitate was obtained immediately after the addition of $KMnO_4$ solution followed by continuous stirring for 5 h. The resultant products were then filtered, washed with distilled water followed by ethanol, and dried at 80 °C for 12 h. Finally, the as-prepared sample was ground using an agate mortar and annealed at 450 °C for 5 h before characterization. For preparing α-MnO_2@C, maleic acid was used as the carbon source. 100 mg α-MnO_2 nanoparticles were added slowly to a 5 mL ethanolic solution of 25 mg maleic acid and stirred at a mild temperature (50 °C) until gel formation was obtained. Then, the obtained gel was heated at 270 °C for 3 h under Ar atmosphere.

The crystalline nature of the powder samples was characterized using X-ray diffraction (XRD, Shimadzu X-ray diffractometer, Chonnam National University, Republic of Korea) with Cu-Kα radiation ($\lambda = 1.54056$ Å) operating at 40 kV and 30 mA over the 2θ range of 10° to 80° in steps of 0.01°. The morphology and elemental distribution of the final products were characterized by scanning electron microscopy (SEM, Hitachi, Chonnam National University, Republic of Korea), field-emission transmission electron microscopy (FE-TEM, Tecnai-F20) with an accelerating voltage of 200 kV, and energy dispersive X-ray (EDX) spectroscopy (EX-200, Hitachi, Chonnam National University, Republic of Korea). For FE-TEM studies, the samples were dispersed in ethanol by ultrasonication before a few drops of the dispersion were put on copper grids and held until the solvent evaporated at room temperature.

Both pristine and carbon-coated MnO_2 electrodes in this study were prepared by mixing the active materials, Ketjen black, and teflonated acetylene black (TAB) with a ratio of 7:2:1, and were then pasted onto a stainless-steel mesh. The prepared cathodes were then vacuum-dried at 120 °C for 12 h. The anode was a Zn metal foil with a thickness of 0.25 mm and 1 M $ZnSO_4$ (pH 4.0) aqueous solution was used as the electrolyte. To assemble 2032-type coin cells, a glass fiber was sandwiched between the cathode and the Zn foil in the electrolyte. The coin cells assembled in an open-air atmosphere were aged overnight before electrochemical measurements. Cyclic voltammetry (CV) was performed at a scan rate of 0.5 mV/s in the voltage range 1.0–1.8 V and electrochemical impedance spectroscopy (EIS) was performed with an amplitude of 5 mV at frequencies varying from 100 mHz to 10 kHz using a Bio Logic Science Instrument (VSP 1075). The electrochemical discharge/charge measurements at room temperature were performed using a BTS 2004H (Nagano Keiki Co. Ltd., Ohta-ku, Tokyo, Japan) analyzer.

3. Results and discussion

In this study, α-MnO_2 was prepared by a simple redox reaction in DI water between manganese acetate and potassium permanganate and the reaction can be described as follows:

$$3Mn(CH_3COO)_2 + 2KMnO_4 + 2H_2O \rightarrow 5MnO_2 + 4CH_3COOH + 2CH_3COOK$$

A dark brown precipitate was formed immediately after the addition of the $KMnO_4$ solution. This simple redox reaction is widely used to prepare MnO_2 nanoparticles. MnO_2 exhibits poor electrical conductivity, thereby limiting electronic transport and hence its performance for electrochemical applications. The techniques of utilizing highly conductive materials such as carbon to improve the electronic transport and hence electrochemical performance in MnO_2 electrodes are well recorded in previous studies. Recently, Li et al. have prepared carbon-coated MnO_2 nanorods by solid-state grinding and annealing at lower temperature using malic acid as the carbon source [6]. In the present study, we have slightly modified that method for preparing carbon-coated MnO_2 by using maleic acid as the carbon source.

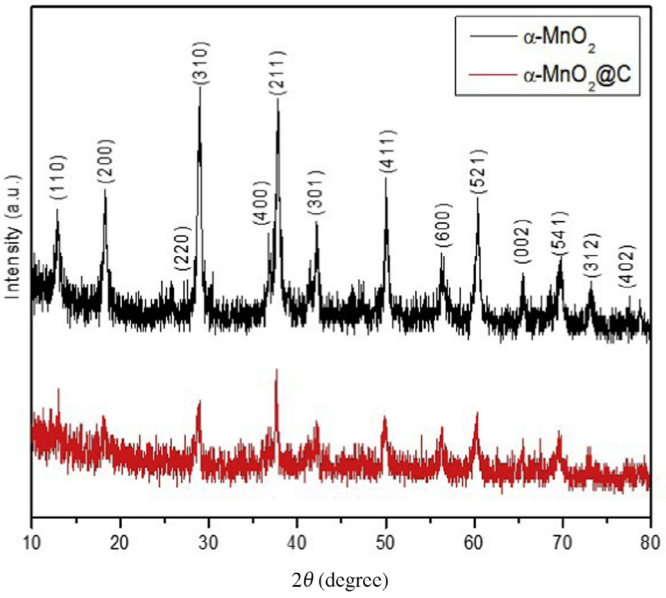

Fig. 1. XRD pattern of the pristine and carbon-coated α-MnO_2 powder.

Fig. 1 shows the XRD patterns for both pristine α-MnO_2 and α-MnO_2@C samples. Both of the patterns match well with the pattern of α-MnO_2 (JSPDS card no. 44-0141). This observation suggests that carbon coating does not influence the structure of α-MnO_2 [10]. The calculated values of the pristine α-MnO_2 unit cell parameters were $a = 9.837$ Å and $c = 2.860$ Å. On the other hand, the lattice parameters of the α-MnO_2@C were $a = 9.731$ Å and $c = 2.814$ Å. The peak intensities appear relatively low for the α-MnO_2@C sample [5,6].

The surface morphologies of the pristine α-MnO_2 and α-MnO_2@C samples were studied using electron microscopy. The FE-SEM images of the pristine α-MnO_2 and α-MnO_2@C are shown in Fig. 2(a) and (b), respectively. Uniform particles with spherical shaped sizes ca. 20 nm for α-MnO_2 and α-MnO_2@C were observed from these images. Similar SEM images were obtained for the pristine α-MnO_2 and α-MnO_2@C, indicating that no obvious change in morphology occurred after carbon coating [6]. Furthermore, in order to investigate the carbon coating, the sample was characterized by FE-TEM as well. The FE-TEM images recorded for α-MnO_2@C at different magnifications are presented in Fig. 2(c) and (d). The relatively dark shade regions appear to indicate the presence of the clustered α-MnO_2@C. The high resolution TEM image presented in Fig. 2(d) displays distinct fringes with interplanar spacing values of approximately 0.49 nm, corresponding to the (200) planes of α-MnO_2 (JCPDS card no. 44-0141). HR-TEM image recorded for α-MnO_2@C also reveals that the nanoparticles are coated with a thin carbon layer.

EDX mapping for the chemical elements in the sample was also performed and the obtained images in Fig. 3 showing the distribution of C, Mn, and O confirm the presence of carbon in the sample. Also, it is worth noting that the carbon distribution is uniformly spread throughout the selected area of study. This observation appears to suggest that the carbon is uniformly wrapped

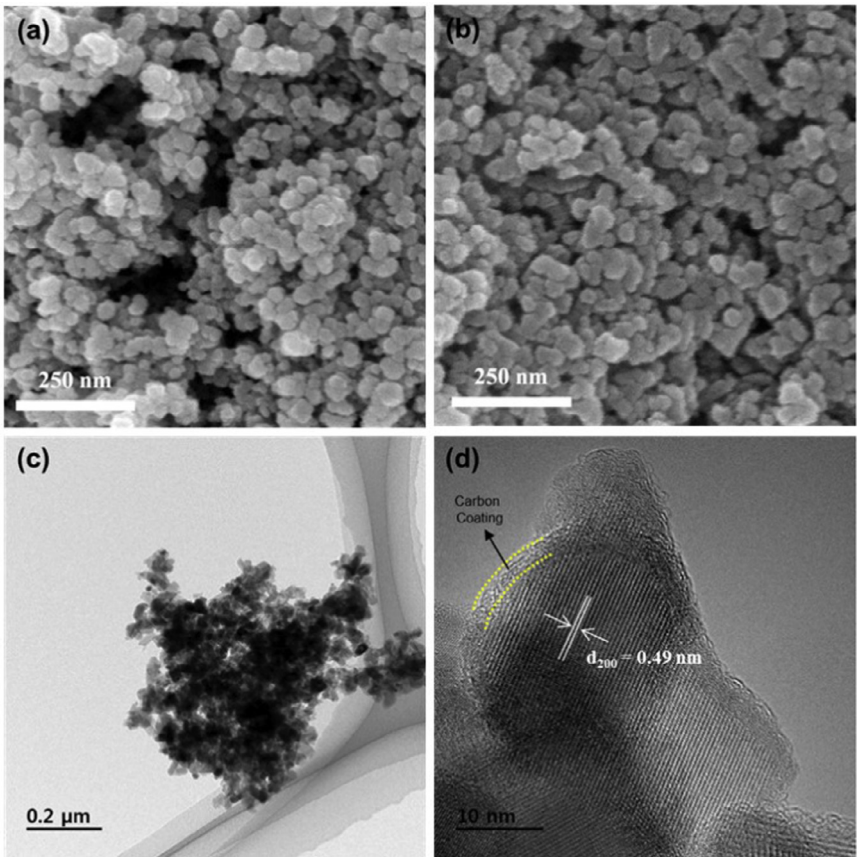

Fig. 2. FE-SEM images of the (a) pristine and (b) carbon-coated α-MnO_2 samples, (c) FE-TEM, and (d) corresponding HR-TEM images of carbon-coated α-MnO_2 sample.

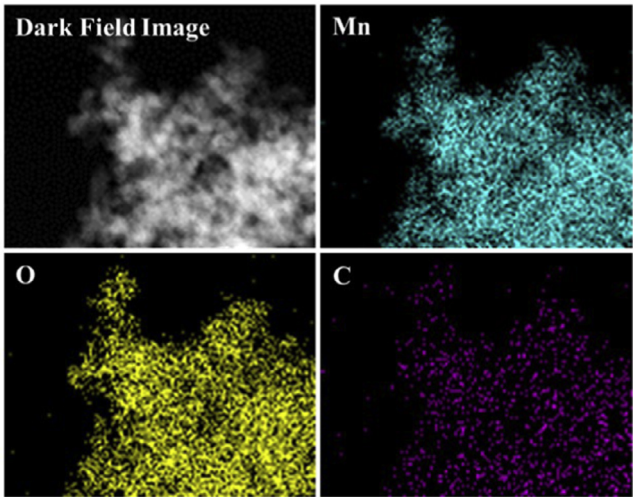

Fig. 3. Elemental image mapping of α-MnO_2@C sample; the dark-field image and corresponding elemental distributions.

on the α-MnO_2 particles. Moreover, the EDX analysis estimated the carbon percentage to be 7.9%, the amount being adequate for carbon network formation. In addition, Raman measurement was also carried out on the carbon-coated α-MnO_2 sample. It can be seen in Fig. S1 that the carbon-coated sample shows two bands at wave numbers around 1375 and 1600 cm^{-1}, corresponding to the D and G band, respectively, indicating the characteristics of carbonaceous compounds. The very low intensity of the D band suggests a higher degree of graphitization of the carbon-coated MnO_2 sample and hence an enhancement its electronic conductivity its expected [15,16]. These results thus validate the chemical synthesis adopted in the present study.

In order to confirm the improved electrochemical properties of α-MnO_2@C as the cathode for ZIB, its electrode performance in a test Zn cell was investigated by CV and electrochemical discharge/charge measurements. Fig. 4(a) shows the CV profiles of the pristine α-MnO_2 and α-MnO_2@C electrodes at a scan rate of 5 mV/s over the potential range 1.0–1.8 V. During the first cycle, two distinct peaks were observed at 1.1 and 1.58 V for the pristine α-MnO_2 electrode and at 1.04 and 1.62 V for α-MnO_2@C. The peaks in the low potential region at 1.1 and 1.0 V for α-MnO_2 and α-MnO_2@C, respectively, can be attributed to the insertion of Zn-ion into the α-MnO_2 host structure, accompanied with the reduction of Mn^{4+} to Mn^{3+}. On the contrary, in the high voltage region, the peaks at 1.58 and 1.62 V for α-MnO_2 and α-MnO_2@C, respectively, correspond to the extraction of Zn-ion, which is involved in the oxidation of Mn^{3+} to its previous state of Mn^{4+} [2,17,18]. During the second scan (Fig. 4(a) inset), two distinct peaks appeared at 1.37 and 1.13 V for Zn-ion insertion into α-MnO_2, whereas peaks at 1.35 and 1.09 V were observed for α-MnO_2@C particles. In the high voltage region, peaks at 1.6 and 1.57 V can be clearly seen for the pristine α-MnO_2 and α-MnO_2@C electrodes, respectively. Compared to the pristine α-MnO_2, α-MnO_2@C exhibits a higher peak intensity and a larger enclosed area of the CV curve, indicating improved electrochemical performance after carbon coating.

Charge/discharge profiles were obtained at a current density of 66 mA/g over the potential range 1.0–1.8 V, as shown in Fig. 4(b). The first discharge capacity for the α-MnO_2@C was 272 mAh/g, whereas the pristine α-MnO_2 registered only 213 mAh/g. It is clear that carbon-coated samples can accommodate more numbers of Zn^{2+} ions than the uncoated MnO_2. In addition, α-MnO_2@C

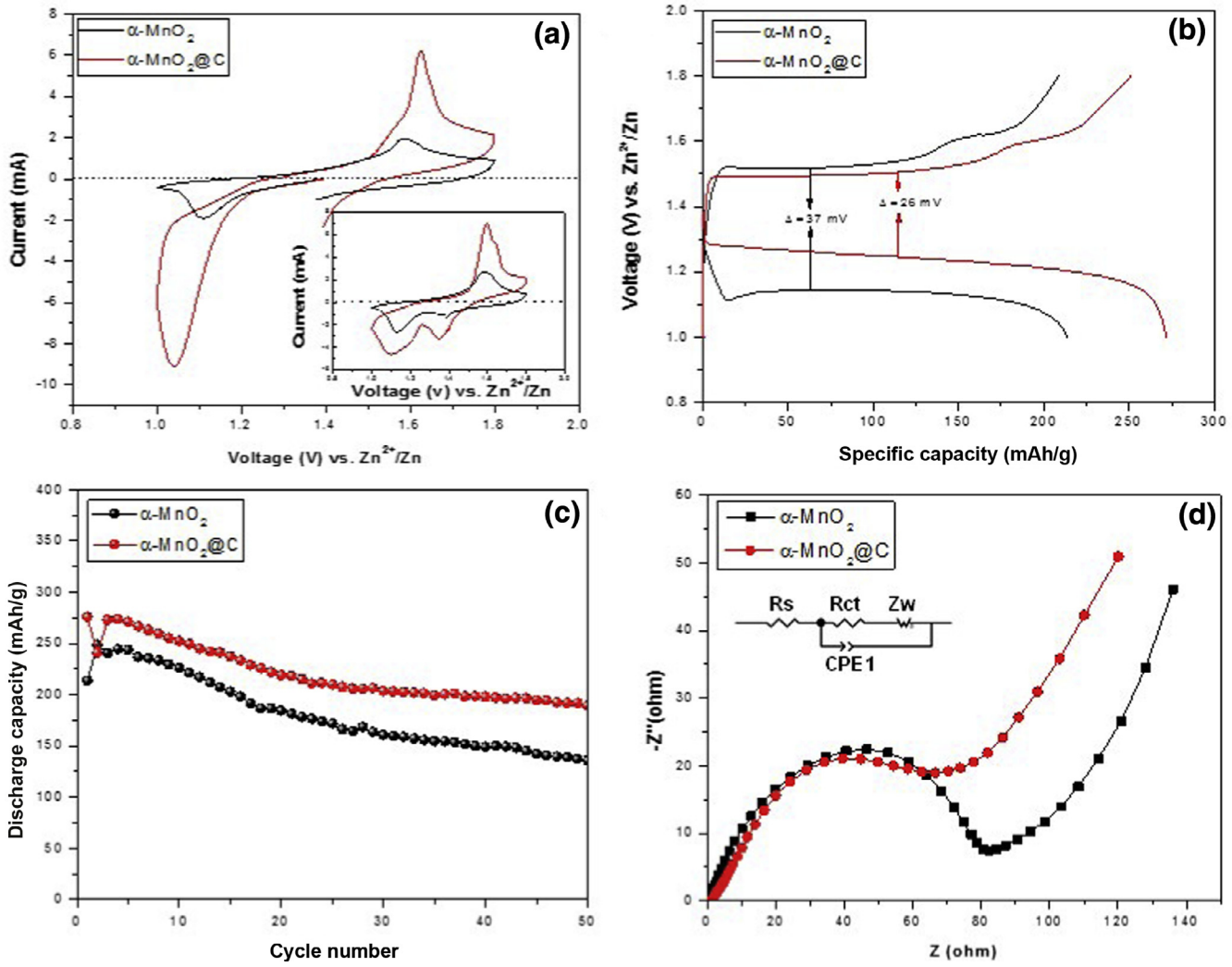

Fig. 4. Cyclic voltammograms of (a) first cycle and (inset) second cycle, (b) discharge/charge voltage profile, (c) cycle performance, and (d) electrochemical impedance spectroscopy of the pristine and carbon-coated MnO_2 samples.

showed a flatter discharge curve than that of α-MnO_2, suggesting a more stable Zn-ion insertion into the α-MnO_2@C sample than in the pristine sample. Furthermore, only a 26 mV polarization value between the discharge and charge plateau was observed for the α-MnO_2@C, whereas it was 37 mV for the pristine α-MnO_2. Zn-ion insertion/extraction into the carbon-coated sample thus more feasible than into the pristine α-MnO_2 sample.

Fig. 4(c) shows the cycling behavior of the α-MnO_2 and α-MnO_2@C electrodes under the current density of 66 mA/g. On long-term cycling, gradual capacity fade is observed for both the electrodes. However, the α-MnO_2@C demonstrated better cycleability than the pristine sample. Precisely, after the 50th cycle, the α-MnO_2@C registered a remarkable discharge capacity of 189 mAh/g, whereas the pristine α-MnO_2 exhibited only 135 mAh/g. Previous studies have reported that the capacity fading of carbon-free MnO_2 electrodes is associated with the increase in the electrode resistance during long-term cycling. Hence, carbon-coated MnO_2 electrodes were used to overcome that problem and increase the conductivity and reduce the resistance with repeated cycling. In addition, previous studies suggested that another reason of capacity fading of MnO_2 electrode in ZIB was the dissolution of Mn in the electrolyte during cycling [19,20]. The carbon coating can effectively prevent manganese dissolution from the MnO_2 electrode during the electrochemical reaction, thereby improving the electrode stability [4,10].

To further confirm the phase transformation during electrochemical Zn-ion insertion, the XPS measurements were conducted on the fresh and discharged state of the carbon-coated α-MnO_2 samples. The Mn $2p_{3/2}$ XPS spectra of the fresh and discharged α-MnO_2@C electrodes were recorded (Fig. S2) and the binding energy of the latter (641.58 eV) being slightly lower than that of the fresh electrode (642.08 eV), indicates that manganese exists in the Mn(III) state [2,17]. In addition, no satellite feature commonly found for Mn(II) state can be observed [21]. These observations indicate that during electrochemical Zn-ion insertion, the manganese is reduced to Mn(III) from Mn(IV) state [2,17].

EIS measurements were performed to evaluate the difference in the electrochemical conductivity between the pristine and carbon-coated α-MnO_2 electrode. As depicted in Fig. 4(d), the Nyquist plots, along with their corresponding equivalent circuit, contain one semicircle and a straight line in the high and low frequency region, respectively. The charge transfer resistance (R_{ct}) value for pristine α-MnO_2 was 81 Ω, and after carbon coating the R_{ct} value reduced to 68 Ω, which indicates the improved electrical conductivity of the carbon-coated sample, i.e., the carbon coating allows a smooth pathway for Zn-ion insertion and extraction. Our present study demonstrates that carbon-coated α-MnO_2 may pave the way for the improvement of MnO_2 electrodes as high performance cathode materials for environmentally benign and cost-effective ZIB applications.

4. Conclusions

In summary, α-MnO_2/C nanoparticles were prepared simply by stirring α-MnO_2 in an ethanolic solution of maleic acid at 50 °C and annealed at 270 °C temperature under Ar atmosphere. When tested in ZIB, the α-MnO_2@C sample registered a prominent discharge capacity of 272 mAh/g, which is higher than the discharge capacity of α-MnO_2 (213 mAh/g). After the 50th cycle, a remarkable discharge capacity of 189 mAh/g was observed for α-MnO_2@C, whereas pristine α-MnO_2 exhibited a discharge capacity of only 135 mAh/g. Moreover, CV analysis established the enhanced electrochemical activity of carbon-coated samples. In addition, the carbon coating improved the conductivity by reducing the charge transfer resistance of the cathode materials, which was confirmed by EIS. The carbon coating not only improved the electrical conductivity but also enhanced the specific capacity and the cycling performance of the α-MnO_2 electrode significantly. Thus, carbon-coated α-MnO_2 appears to be a very promising candidate for further application in environmentally benign ZIBs.

Acknowledgments

This work was supported by the National Research Foundation of Korea (NRF) grant funded by the Korea government (MSIP) (2014R1A2A1A10050821).

Supplementary materials

Supplementary material associated with this article can be found, in the online version, at doi:10.1016/j.jechem.2017.04.002.

References

[1] S. Deravaj, N. Munichandraiah, J. Phys. Chem. C 112 (2008) 4406–4417.
[2] M.H. Alfaruqi, J. Gim, S. Kim, J. Song, J. Jo, S. Kim, V. Mathew, J. Kim, J. Power Sources 288 (2015) 320–327.
[3] J. Lee, J.B. Ju, W. Cho, B. Cho, S. Oh, Electrochim. Acta 112 (2013) 138–143.
[4] D. Xu, B. Li, C. Wei, Y.-B. He, H. Du, X. Chu, X. Qin, Q.-H. Yang, F. Kang, Electrochim. Acta 133 (2014) 254–261.
[5] A.M. Hashem, A.M. Abdel-Latif, H.M. Abuzeid, H.M. Abbas, H. Ehrenberg, R.S. Farag, A. Mauger, C.M. Julien, J. Alloys Compd. 509 (2011) 9669–9674.
[6] L. Li, X. Guo, F. Hao, X. Zhang, J. Chen, New J. Chem. 39 (2015) 4731–4736.
[7] P. Ning, X. Duan, X. Ju, X. Lin, X. Tong, X. Pan, T. Wang, Q. Li, Electrochim. Acta 210 (2016) 754–761.
[8] J.-G. Wang, Y. Yang, Z.-H. Huang, F. Kang, Mater. Lett. 72 (2012) 18–21.
[9] J.-W. Wang, Y. Chen, B.-Z. Chen, J. Alloys Compd. 688 (2016) 184–197.
[10] A.M. Hashem, H.M. Abuzeida, K. Nikolowski, H. Ehrenberg, J. Alloys Compd. 497 (2010) 300–303.
[11] Y. Hou, Y. Cheng, T. Hobson, J. Liu, Nano Lett. 10 (2010) 2727–2733.
[12] G. Wang, Y. Liu, G. Shao, L. Kong, W. Gao, ACS Sustainable Chem. Eng. 2 (2014) 2191–2197.
[13] Y. Pan, Z. Mei, Z. Yang, W. Zhang, B. Pei, H. Yao, Chem. Eng. J. 242 (2014) 397–403.
[14] I.-T. Kim, N. Kouda, N. Yoshimoto, M. Morita, J. Power Sources 298 (2015) 123–129.
[15] M. Saravanan, M. Ganesan, S. Ambalavanan, J. Power Sources 251 (2014) 20–29.
[16] M.M. Doeff, J.D. Wilcox, R. Kostecki, G. Lau, J. Power Sources 163 (2006) 180–184.
[17] C. Xu, B. Li, H. Du, F. Kang, Angew. Chem. Int. Ed. 51 (2012) 933–935.
[18] J. Lee, J.B. Ju, W. Cho, B. Cho, S. Oh, Electrochim. Acta 112 (2013) 138–143.
[19] M.H. Alfaruqi, V. Mathew, J. Gim, S. Kim, J. Song, J.P. Baboo, S.H. Choi, J. Kim, Chem. Mater. 27 (2015) 3609–3620.
[20] H. Pan, Y. Shao, P. Yan, Y. Cheng, K.S. Han, Z. Nie, C. Wang, J. Yang, X. Li, P. Bhattacharya, K.T. Mueller, J. Liu, Nat. Energy 1 (2016) 16039–16046.
[21] M.C. Biesinger, B.P. Payne, A.P. Grosvenord, L.W.M. Lau, A.R. Gerson, R.S.C. Smart, App. Surf. Sci. 257 (2011) 2717–2730.